



Cite this: *Mater. Adv.*, 2025,
6, 547

Received 26th August 2024,
Accepted 17th November 2024

DOI: 10.1039/d4ma00854e

rsc.li/materials-advances

Strong and stable adhesion of conductive layers on substrates is crucial for the operation and performance of electronic devices, and several attempts have been made to achieve this goal. We report all inkjet-printed electrodes with strong and stable adhesion between conductive layers and flexible polyether sulfone substrates, where ink based on silver nanoparticles was used for metal layers and dielectric ink for intermediate adhesion layers. Quantitative measurements of adhesion properties using an adhesion test and convex tensile bending test revealed negligible and limited resistance changes, respectively. The strong adhesion properties indicated that all inkjet printed Ag electrodes are highly suitable for applications in wearable devices and flexible displays.

Introduction

Printed electronics are recognized as an emerging technology owing to their cost-effectiveness, flexibility, lightweight nature, rapid prototyping capabilities, customization potential, environmental friendliness, and compatibility with diverse materials.^{1–4} These benefits facilitate the adoption of printed electronics technology in various fields, including interconnects,^{5–8} sensors,^{9–13} transistors,^{14,15} antennas,^{16,17} and energy storage.¹⁸ Moreover, the ongoing advancement of this technology is broadening its range of applications.^{19–24} Jing *et al.* developed freestanding functional structures comprising polyimide and silver (Ag) (printed using aerosol-jet technology) intended for use as interconnects in stretchable electronics and sensing applications.⁶ Fu *et al.* reported all-inkjet-printed bimodal sensors capable of simultaneously sensing bending strain and pressure, using Ag nanoparticles (NPs) ink as the conductive material.¹¹ Makhinia *et al.* implemented organic electrochemical transistors capable of fast switching response, printed using a combination of screen and aerosol-jet printing.²²

IT Materials & Components Research Center,
Gumi Electronics & Information Technology Research Institute (GERI),
Cheondangjeop1-ro 17, Sandong-eup, Gumi, Gyeongbuk, Korea.

E-mail: junhee.kim@geri.re.kr

† Electronic supplementary information (ESI) available. See DOI: <https://doi.org/10.1039/d4ma00854e>

Improved adhesion of printed Ag electrodes for flexible transparent display applications†

Han-Jung Kim, Se Yong Park, Jeongmin Park, Yohan Ko, Sung Eun Park, Yoonkap Kim and Junhee Kim *

Furthermore, Zhou *et al.* produced radio frequency passive devices, including an oscillator, power amplifier, and antenna through the direct writing of an Ag ink.¹⁷ The commonality among the aforementioned developments is that they are implemented on flexible or stretchable substrates, demonstrating that printing technologies including aerosol-jet, direct writing, and inkjet, hold promise for expanding the horizon of the industry.

Most electronic devices are implemented with a multi-layer structure to enable operations tailored to their specific purposes. The adhesion between layers considerably impacts the stability, reliability, and performance of devices, making interfacial engineering a crucial issue, and various research efforts are underway to achieve strong adhesion.^{25–27} Cho *et al.* reported enhanced adhesion properties between a copper electrode and a flexible substrate induced by a flash-light sintering process, resulting in mechanical interlocking between them.²⁵ Labiano *et al.* performed plasma treatment to improve adhesion between a graphene ink and a Kapton substrate to fabricate an antenna, with the plasma treatment increasing the wettability of the substrate and making the surface hydrophilic.²⁶ Labiano *et al.* proposed a new method for low-cost and simple fabrication of embedded metal mesh flexible transparent electrodes.²⁷ They ensured mechanical stability by spin-coating liquid polydimethylsiloxane on a polyethylene terephthalate substrate, followed by the direct printing and sintering ultra thin metal mesh on top of it.

In this study, we propose all inkjet-printed double-layer (DL) electrodes featuring adhesion and Ag layers on polyether sulfone (PES) substrates. The adhesion layer was directly printed on the PES substrate using dielectric ink, and the Ag layer on top was printed using AgNP-based ink. To improve the adhesion between the PES substrate and the Ag layer, we inserted a single adhesion layer, achieving enhanced bonding with a simple, continuous process rather than requiring multiple, independent steps as seen in previous approaches.^{25,26} The adhesion test and bending test were implemented. The results indicate that the DL electrodes exhibited negligible and limited

resistance changes, respectively. The findings of our study indicate that the proposed electrode is structurally robust and suitable for the implementation of various devices based on flexible substrates.

Results and discussion

We evaluated two structures of Ag electrodes: a single-layer (SL) electrode with a 25 μm Ag layer directly printed on the PES substrate and a DL electrode consisting of a 5 μm dielectric ink adhesion layer and a 25 μm Ag layer, both printed on the PES substrate, as depicted in Fig. 1a (refer to ESI[†] for further details). Although the electrodes were designed with right-angled edges, the nature of the inkjet printing process resulted in a dome-shaped profile owing to the surface tension of the ink droplets.^{28–30}

Fig. 1b shows the changes in resistance as a function of the number of the adhesion tests performed on the SL and DL electrodes. The adhesion tests were conducted using 3M Scotch 610 tape, as specified in ASTM-D3359 (refer to ESI[†] for further details), and were performed a total of 15 times. While the resistance of the SL electrode increased to an unmeasurable point after only one adhesion test, the DL electrode exhibited virtually no change even after 15 adhesion tests (refer to Fig. S1 for the results of the adhesion test performed on the SL electrode ESI[†]). This indicates that the adhesion layer inserted between the PES substrate and Ag layer was effectively fulfilling

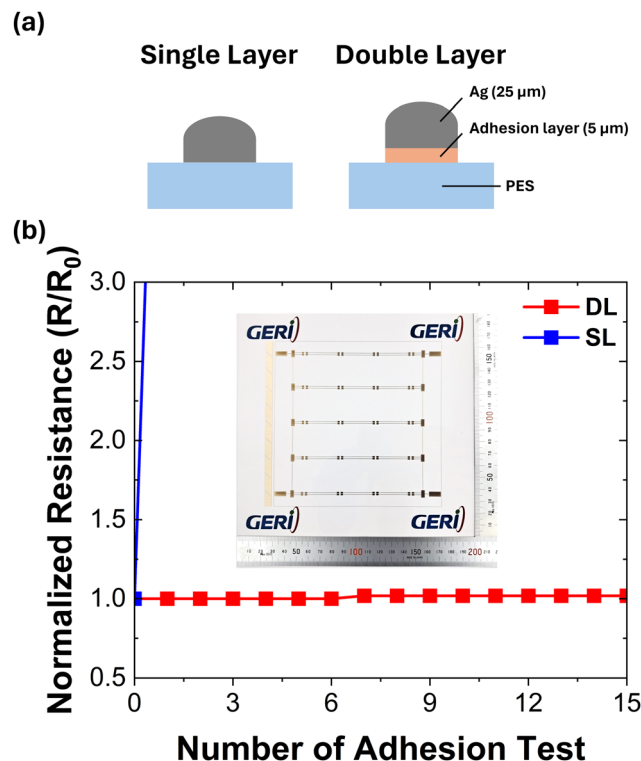


Fig. 1 (a) Electrode structures, exhibiting SL and DL electrodes. (b) Resistance measurement results indicating the change in resistance relative to the initial resistance as a function of the number of adhesion tests on the DL electrode. (Inset: image of a circuit printed on a PES substrate.)

its role. The inset of Fig. 1b shows a sample of the circuit printed on the transparent PES substrate used in this study, with a sufficiently large area to be applicable to various devices.

To assess the potential application of the proposed electrode in the field of flexible printed electronics, tensile bending tests, also referred to as convex bending tests, were performed. The tests were designed to induce mechanical stress by bending the samples in a manner that increases the distance between AgNPs. These tests comprised 1000 cycles of bending at radii of 4.0, 4.5, and 5.0 mm. Fig. 2a shows the normalized change in the resistance of the SL electrode, and Fig. 2b shows the corresponding results for the DL electrode, comparing resistance changes as a function of the bending tests (refer to Fig. S1 for the results of the concave bending tests ESI[†]).

For the SL electrode, the resistance change was minimal at a bending radius of 5.0 mm. At 4.5 mm, a substantial increase in resistance was observed after approximately 700 cycles. At 4.0 mm, substantial resistance changes were detected from the initial stage of the test. The increased resistance changes at

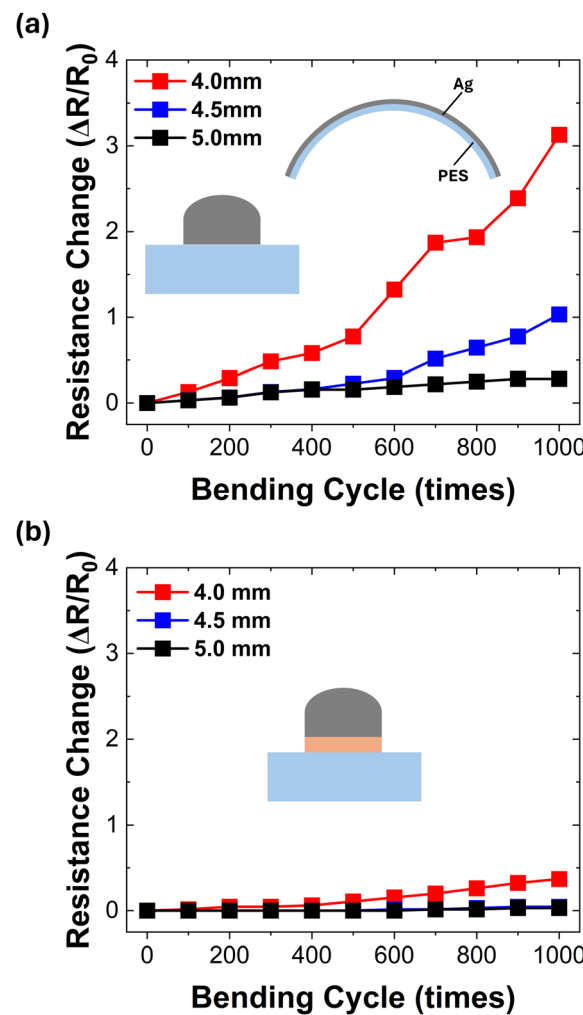


Fig. 2 Normalized change in resistance as a function of the 1000 cycles of the convex tensile bending tests conducted at radii of 4.0, 4.5, and 5.0 mm for (a) the SL and (b) DL electrodes.



smaller radii can be attributed to higher mechanical stress imposed on the structure.

By contrast, the DL electrode exhibited exceptional stability. At bending radii of 5.0 and 4.5 mm, the resistance change was negligible. Even at a radius of 4.0 mm, the resistance change was limited to approximately 37%, which is markedly lower compared to the 313% change observed in the SL electrode under identical conditions. This considerable difference may be attributed to the adhesion layer in the DL electrode, which enhances the interface between the PES and Ag, thereby improving mechanical robustness and stress tolerance.

Fig. 3 shows a comparative analysis of the SL and DL electrodes subjected to 1000 cycles of convex tensile bending tests to comprehensively evaluate the durability of the electrodes. The results are illustrated through a series of images.

Optical microscope (OM) images in Fig. 3a and d show the initial states of the SL and DL electrodes before the tensile bending test. The SL electrode shown in Fig. 3b exhibits substantial structural damage and cracks after 1000 cycles of tensile bending, highlighting the impact of mechanical stress. The scanning electron microscope (SEM) image in Fig. 3c of the red-boxed area illustrated in Fig. 3b reveals severe mechanical failure, including the detachment of Ag flakes from the PES substrate.

By contrast, the DL electrode exhibits remarkable stability under the same testing conditions. Fig. 3d shows the initial state of the DL electrode, and Fig. 3e shows the structure after the tensile bending test. The DL electrode maintains its integrity, with minimal visible damage. The SEM image in Fig. 3f of the red-boxed area illustrated in Fig. 3e further confirms the preservation of the structure with only minor cracks. This performance underscores the effectiveness of the adhesion layer in enhancing mechanical robustness. Fig. 3g illustrates the tensile bending test setup applied to the SL and DL electrodes, indicating the direction and nature of the mechanical stress imposed.

These findings indicate that the DL electrode is more suitable for applications in flexible printed electronics where mechanical reliability is crucial. The enhanced durability exhibited by the adhesion layer indicates that the DL electrode can better withstand the mechanical demands of flexible electronic devices, making it a more viable option for future applications.

As shown in Fig. 4a, a circuit is printed on a transparent PES substrate. The printed circuit covers an area of approximately $140 \times 140 \text{ mm}^2$, which is a considerable size suitable for various device applications, such as large-scale flexible displays and wearable electronics. The use of PES as a substrate highlights its flexibility and suitability for applications requiring durability and transparency.

Fig. 4b and c demonstrate the practical application of the DL electrode. Fig. 4b shows the flexible display operating normally with LEDs mounted on a flexible PES substrate without any deformation. This indicates that the DL electrode can maintain functionality under standard conditions. Fig. 4c illustrates that the flexible display continues to function correctly even when the flexible PES substrate is bent, demonstrating the durability and flexibility of the DL electrode (refer to the video provided in ESI†). These results indicate that the DL electrode is highly suitable for use in flexible electronics, such as flexible displays, sensors, and wearable devices.

Conclusions

In summary, this study demonstrates the advantages of DL electrodes in flexible electronics, using a combination of dielectric ink and AgNP ink. It reveals the superior adhesion and mechanical robustness of DL electrodes compared with those of SL electrodes. The adhesion test indicated that the DL electrode exhibited negligible resistance change, confirming effective adhesion. Convex tensile bending tests involving 1000 repetitive cycles at various radii further indicated the exceptional stability and minimal resistance changes of the

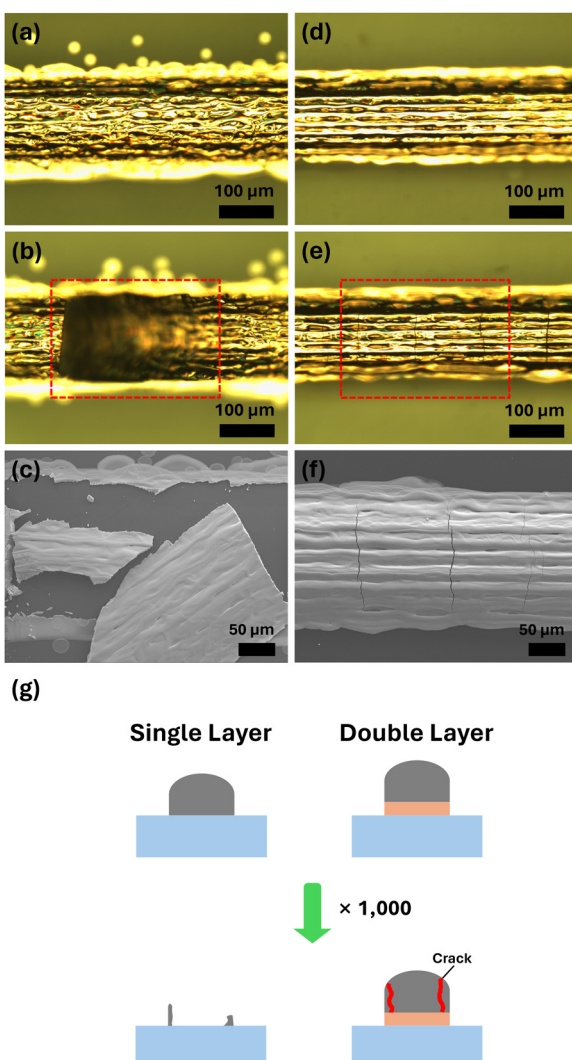


Fig. 3 (a) and (d) OM images of SL and DL electrodes, respectively, before the tensile bending test. (b) and (e) OM images of SL and DL electrodes, respectively, after the tensile bending test. (c) and (f) SEM images of the regions marked with red-boxes in (b) and (e), respectively, providing detailed observations of the structures after the bending test. (g) Tensile bending test applied to both SL and DL electrodes.



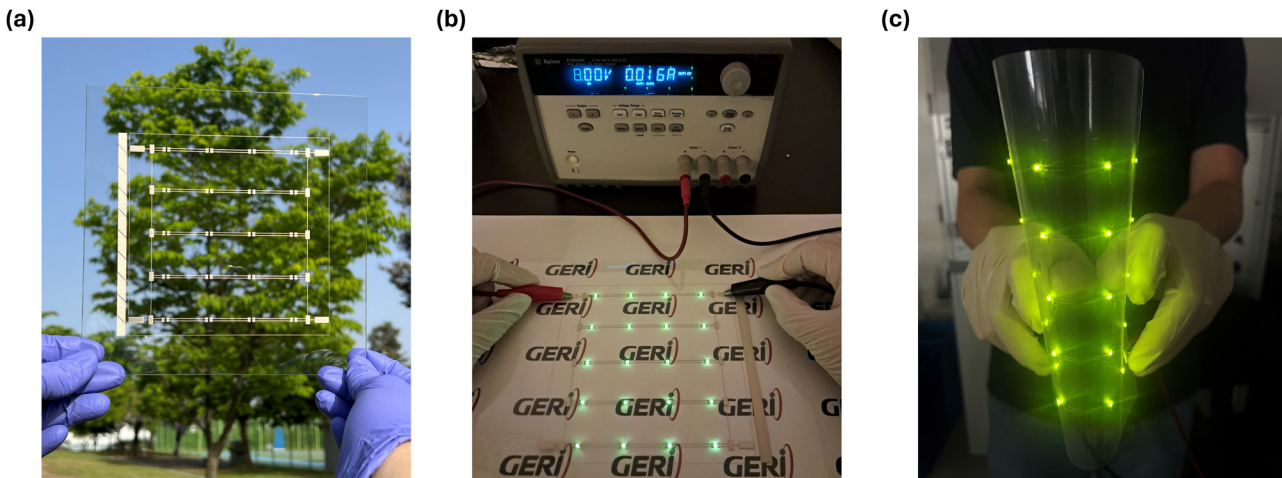


Fig. 4 (a) Circuit printed on a transparent PES substrate. (b) Operation of a flexible display with mounted LEDs without bending. (c) Operation of a flexible display with mounted LEDs under bending.

DL electrodes, whereas the SL electrodes experienced substantial mechanical failure. OM and SEM images provided detailed insights into the structural stability, indicating minimal damage in the DL electrodes. The adhesion layer is crucial for enhancing mechanical bonding and overall durability, making DL electrodes highly suitable for flexible electronics such as wearable devices and flexible displays. The ability to print on flexible and rigid substrates without sacrificing performance demonstrates the potential of this approach in advancing the field of printed electronics, paving the way for more reliable and durable flexible electronic devices. Furthermore, future studies will focus on incorporating self-healing techniques and enhancing flexibility to address electrode cracking. These advancements are expected to be applicable in various fields, including flexible and rollable displays, flexible sensors, and wearable devices.

Author contributions

H.-J. Kim: conceptualization, data curation, formal analysis, investigation, methodology, validation, S. Y. Park: conceptualization, data curation, writing – original draft, review & editing, J. Park: resources, investigation, methodology, Y. Ko: writing – review & editing, S. E. Park: writing – review & editing, Y. Kim: writing – review & editing, J. Kim: conceptualization, formal analysis, methodology, visualization, writing – original draft, review & editing.

Data availability

The data supporting this article have been included as part of the ESI.†

Conflicts of interest

The authors declare no conflicts of interest.

Acknowledgements

This work was supported by the Korea Innovation Foundation (INNOPOLIS) grant funded by the Korea government (MSIT) (2020-DD-UP-0278). We would like to thank Editage (<https://www.editage.co.kr>) for pre-submission English language editing.

References

- 1 H.-J. Kim and Y. Kim, *Micro Nano Syst. Lett.*, 2021, **9**, 6.
- 2 H.-J. Kim, D.-I. Choi, S. Lee, S.-K. Sung, D.-H. Kang, J. Kim and Y. Kim, *Adv. Electrode Mater.*, 2021, **23**, 2100395.
- 3 T. Kamijo, S. d Winter, P. Panditha and E. Meulenkamp, *ACS Appl. Electron. Mater.*, 2022, **4**, 698–706.
- 4 H. Liu, X. Yin, C. Chi, T. Feng, P. Wang, W. Wang and H. Tian, *ACS Appl. Electron. Mater.*, 2024, **6**, 724–736.
- 5 Y.-G. Park, H. S. An, J.-Y. Kim and J.-U. Park, *Sci. Adv.*, 2019, **5**, eaaw2844.
- 6 Q. Jing, Y. S. Choi, M. Smith, C. Ou, T. Busolo and S. Kar-Narayan, *Adv. Mater. Technol.*, 2019, **4**, 1900048.
- 7 A. D. Valentine, T. A. Busbee, J. W. Boley, J. R. Raney, A. Chortos, A. Kotikian, J. D. Berrigan, M. F. Durstock and J. A. Lewis, *Adv. Mater.*, 2017, **29**, 1703817.
- 8 Y.-T. Kwon, Y.-S. Kim, S. Kwon, M. Mahmood, H.-R. Lim, S.-W. Park, S.-O. Kang, J. J. Choi, R. Herbert, Y. C. Jang, Y.-H. Choa and W.-H. Yeo, *Nat. Commun.*, 2020, **11**, 3450.
- 9 F. L. Goupil, G. Payrot, S. Khiev, W. Smaal and G. Hadzioannou, *ACS Omega*, 2023, **8**, 8481–8487.
- 10 Z. J. Khattak, M. Sajid, M. Javed, H. M. Z. Rizvi and F. S. Awan, *ACS Omega*, 2022, **7**, 16605–16615.
- 11 S. Fu, J. Tao, W. Wu, J. Sun, F. Li, J. Li, Z. Huo, Z. Xia, R. Bao and C. Pan, *Adv. Mater. Technol.*, 2019, **4**, 1800703.
- 12 T. Lee, Y. Kang, K. Kim, S. Sim, K. Bae, Y. Kwak, W. Park, M. Kim and J. Kim, *Adv. Mater. Technol.*, 2022, **7**, 2100428.
- 13 D. Barmpakos, V. Belessi, R. Schelwald and G. Kaltsas, *Nanomaterials*, 2021, **11**, 2025.



14 T. N. Mangoma, S. Yamamoto, G. G. Malliaras and R. Daly, *Adv. Mater. Technol.*, 2022, **7**, 2000798.

15 T. Carey, A. Arbab, L. Anzi, H. Bristow, F. Hui, S. Bohm, G. Wyatt-Moon, A. Flewitt, A. Wadsworth, N. Gasparini, J. M. Kim, M. Lanza, I. McCulloch, R. Sordan and F. Torrisi, *Adv. Electron. Mater.*, 2021, **7**, 2100112.

16 G. McKerricher, D. Titterington and A. Shamim, *IEEE Antennas Wirel. Propag. Lett.*, 2016, **15**, 544–547.

17 N. Zhou, C. Liu, J. A. Lewis and D. Ham, *Adv. Mater.*, 2017, **29**, 1605198.

18 P. K. Katkar, S. J. Marje, V. G. Parale, C. D. Lokhande, J. L. Gunjakar, H.-H. Park and U. M. Patil, *Langmuir*, 2021, **37**, 5260–5274.

19 E. F. Gomez, S. V. Wanasinghe, A. E. Flynn, O. J. Dodo, J. L. Sparks, L. A. Baldwin, C. E. Tabor, M. F. Durstock, D. Konkolewicz and C. J. Thrasher, *ACS Appl. Mater. Interfaces*, 2021, **13**, 28870–28877.

20 P. Zhang, I. M. Lei, G. Chen, J. Lin, X. Chen, J. Zhang, C. Cai, X. Liang and J. Liu, *Nature*, 2022, **13**, 4775.

21 J. D. Hubbard, R. Acevedo, K. M. Edwards, A. T. Alsharhan, Z. Wen, J. Landry, K. Wang, S. Schaffer and R. D. Sochol, *Sci. Adv.*, 2021, **7**, eabe5257.

22 A. Makhinia, K. Hübscher, V. Beni and P. A. Ersman, *Adv. Mater. Technol.*, 2022, **7**, 2200153.

23 Q. Li, J. Zhang, Q. Li, G. Li, X. Tian, Z. Luo, F. Qiao, X. Wu and J. Zhang, *Front. Mater.*, 2019, **5**, 1–14.

24 K. A. Nirmal, T. D. Dongale, A. C. Khot, C. Yao, N. Kim and T. G. Kim, *Nano-Micro Lett.*, 2024, **17**, 1–17.

25 C. H. Cho, I. K. Shin, K. Y. Kim and Y. J. Choi, *Appl. Surf. Sci.*, 2019, **485**, 484–489.

26 I. I. Labiano and A. Alomainy, *Flex. Print. Electron.*, 2021, **6**, 025010.

27 Z. Li, H. Li, X. Zhu, Z. Peng, G. Zhang, J. Yang, F. Wang, Y. Zhang, L. Sun, R. Wang, J. Zhang, Z. Yang, H. Yi and H. Lan, *Adv. Sci.*, 2022, **9**, 2105331.

28 M. Cinquino, C. T. Prontera, A. Zizzari, A. Giuri, M. Pugliese, R. Giannuzzi, A. G. Monteduro, M. Carugati, A. Banfi, S. Carallo, A. Rizzo, A. Andretta, G. Dugnani, G. Gigli and V. Maiorano, *J. Sci.: Adv. Mater. Devices*, 2022, **7**, 100394.

29 Y. Li, L. Lan, S. Sun, Z. Lin, P. Gao, W. Song, E. Song, P. Zhang and J. Peng, *ACS Appl. Mater. Interfaces*, 2017, **9**, 8194–8200.

30 D. Kim, S. Jeong, B. K. Park and J. Moon, *Appl. Phys. Lett.*, 2006, **89**, 264101.

